engineering proceedings

MDPI

Proceeding Paper

On the Sensitivity of the Daily Maximum and Minimum Air Temperature of Egypt to Soil Moisture Status and Land Surface Parameterization Using the RegCM4 †

Samy Ashraf Anwar * and Sally Mahmoud Mostafa

Egyptian Meteorological Authority, Qobry EL-Kobba, Cairo P.O. Box 11784, Egypt; sally.mahmoud_2014@yahoo.com

* Correspondence: ratebsamy@yahoo.com

† Presented at the 4th International Electronic Conference on Applied Sciences, 27 October–10 November 2023; Available online: https://asec2023.sciforum.net/.

Abstract: Daily maximum (TMX) and minimum air temperature (TMN) are sensitive to the soil moisture status and land surface parameterization. However, this point has not been addressed in arid regions (e.g., Egypt). To address this issue, four 13-year simulations were conducted within the framework of the regional climate model (RegCM4). The first two considered the soil moisture status (bare soil versus global satellite soil moisture product; ESACCI). The other two considered the sensitivity to the two land surface schemes coupled to the RegCM4: Biosphere Atmosphere Transfer System (BATS) and version 4.5 of the community land model (CLM45). In all simulations, the RegCM4 was downscaled by the Era-Interim reanalysis with 25 km grid spacing. The simulated TMX and TMN were evaluated with respect to the Climate Research Unit (CRU) and station data. The results showed that switching from bare soil to ESACCI has a considerable influence on the simulated TMX and TMN. Compared to the CRU, the CLM45 outperforms the BATS in the coasts of the Mediterranean and Red Sea (concerning the TMX) and in the inland regions (regarding the TMN). In comparison with the station data, behavior of the BATS/CLM45 varies with the location and month. Despite of the noted biases, the RegCM4 can be recommended for future studies concerning the seasonal forecast or climate change of Egypt when it is configured with the CLM45 land surface model and initialized with the ESACCI satellite product.

Keywords: BATS; CLM45; Egypt; ESACCI; RegCM4

Citation: Anwar, S.A.; Mostafa, S.M. On the Sensitivity of the Daily Maximum and Minimum Air Temperature of Egypt to Soil Moisture Status and Land Surface Parameterization Using the RegCM4. *Eng. Proc.* **2023**, *52*, x. https://doi.org/10.3390/xxxxx

Academic Editor(s): Name

Published: date

1. Introduction

Soil moisture plays an important role in controlling the terrestrial hydrological cycle as well as the whole climate system [1, 2]. Indeed, soil moisture controls the surface energy balance and climate through changes of the water vapor transferred to the atmosphere from soil evaporation and vegetation transpiration [3]. As a result, it determines the total evapotranspiration budget and eventually the degree of cooling/warming of the atmosphere. Additionally, soil moisture can affect the status of the vegetation cover (represented by the leaf area index; [4]) and the terrestrial carbon fluxes through changes in the photosynthesis rate, leaf carbon. In fact, the aforementioned effects of the soil moisture (either on the surface climate or the terrestrial carbon fluxes) have been documented using regional climate models.

For instance, the authors of [3] used the International Center of Theoretical Physics regional climate model (RegCM4; [5]) to investigate the possible effects of the soil moisture changes (represented by the runoff schemes of the version 4.5 of the community land model; CLM45 [6]) on the surface energy balance and climate with respect to various reanalysis products. They reported that soil moisture changes considerably affect the

total evapotranspiration budget and therefore the surface climate (represented by the mean air temperature and total surface precipitation). In fact, the influence of soil moisture on the surface climate, daily air maximum and minimum air temperature has been investigated in various regions across the globe [7–9]. Moreover, soil moisture has a considerable influence on the global incident solar radiation [10], terrestrial carbon fluxes [11,12] and potential evapotranspiration (PET; [13]).

Role of the land surface parameterization (in simulating the surface climate) has been investigated using regional climate models (e.g., RegCM4). Indeed, the land surface parameterization differs in representing the soil moisture dynamics as well as the initialized values of the soil moisture of each scheme. For instance, the authors of [14] reported that version 3.5 of the community land model (CLM35; [15]) is initially wetter than the Biosphere Atmosphere Transfer system (BATS; [16]). Furthermore, the simple representation of the BATS (compared to the CLM35) leads to higher soil moisture accumulated on the surface and therefore lower temperature and higher total surface precipitation than the one noted in the CLM35. Additionally, they reported that CLM35 outperforms the BATS in comparison with reanalysis products. The same behavior has been noted in the comparison between the BATS and CLM45 [17,18].

It should be noted that the aforementioned literature reviews investigated the possible influences of the soil moisture changes either by different land surface schemes or different runoff schemes of the same land surface model in wet regions (i.e., with a surplus of soil moisture). Concerning possible influences in arid regions (e.g., Middle East and North Africa; MENA), the authors of [19] reported that representation of the soil moisture changes (by adapting different land surface schemes) lead to a different response of the radiation budget or surface climate variables. They concluded that caution must be taken to ensure appropriate selection of the suitable land surface scheme for the regional climate simulation.

However, sensitivity of the surface climate to the status of the soil moisture initialization (i.e., bare soil versus satellite soil moisture product) in arid regions has not been examined till the present day. Additionally, sensitivity of the surface climate to different land surface schemes (considering the satellite soil moisture product as an initial condition of the soil moisture) has not been addressed yet in arid regions (e.g., Egypt). Therefore, the present study aims to:

1. Examine the sensitivity of the daily maximum (TMX) and minimum air temperature (TMN) of Egypt to the status of the soil moisture initialization (bare soil versus ESACCI global satellite soil moisture product; [20,21]) using the RegCM4.
2. Study the role of land surface parameterization (BATS versus CLM45) in simulating the daily TMX and TMN of Egypt with respect to the Climate Research Unit (CRU; [22]) considering the ESACCI as an initial condition of the soil moisture.
3. Evaluate the climatological annual cycle of the TMX and TMN with respect to the station observations.

Section 2 describes the materials and methods used in this study; Section 3 shows the results of the study. Section 4 provides the discussion and conclusion.

2. Materials and Methods

2.1. Model Description and Experiment Design

In the present study, we used version 4.7 of the International Center of Theoretical Physics regional climate model (RegCM; [5]). The authors of [5] reported that RegCM4 includes an improved version of the physical parameterization compared with its preceding version (RegCM3; [23]). The RegCM4 adopts its dynamical core from the fifth version of Pennsylvania State University Mesoscale Model (MM5, [24]). Recently, a new non-hydrostatic core has been implemented in the RegCM's code (RegCM5; [25]). In addition, the RegCM4's code has been modified to read the ESACCI global satellite soil moisture product as an initial condition of the soil moisture. Concerning the land surface

parameterization, three land surface models have been coupled to the RegCM4 to control the lower initial condition of the atmosphere: 1—BATS [16], 2—CLM35 [15] and 3—CLM45 [6]. For the purpose of the present study, only BATS and CLM45 were selected.

The RegCM4's domain was centered at latitude 27° and longitude 30° with 60 points in the zonal and meridional directions following [26]. Additionally, the RegCM4 was downscaled by the Era-Interim reanalysis of 1.5 degrees (EIN15) with 25 km horizontal grid spacing following [27, 28]. To ensure an optimized performance of the RegCM4 in the present study, the physical configuration of [28] was considered. The reader can refer to [29] for more details concerning the climatic features of Egypt. The authors of [27] reported that the RegCM4 gives a similar either if it is downscaled by the EIN15 or the NCEP/NCAR reanalysis version 2 of 2.5 degrees (NNRP2; [30]). Therefore, EIN15 was used in the present study to provide the lateral boundary condition and sea surface temperature.

To address the purpose of the present study, four 13-year simulations (1998–2010) were conducted. The four simulations were divided to two groups. The first group considered the sensitivity of the TMX and TMN to the status of the initialized soil moisture either from the bare soil or from the ESACCI satellite soil moisture product. On the other hand, the second group discusses the sensitivity of the simulated TMX/TMN to the land surface parameterization (BATS and CLM45). It is important to mention that in the second group, the RegCM4 was initialized with the ESACCI for two reasons: 1—performance of the CLM45 is similar to the BATS when the RegCM4 is initialized from bare soil (not shown) and 2—performance of BATS/CLM45 differs with initialized values of the soil moisture as reported by [14].

In the four simulations, the first three years were considered as spin-up so the simulated soil moisture can approach an equilibrium state following [13,14]. Figure 1 shows the interpolated ESACCI on the curvilinear grid of the RegCM4.

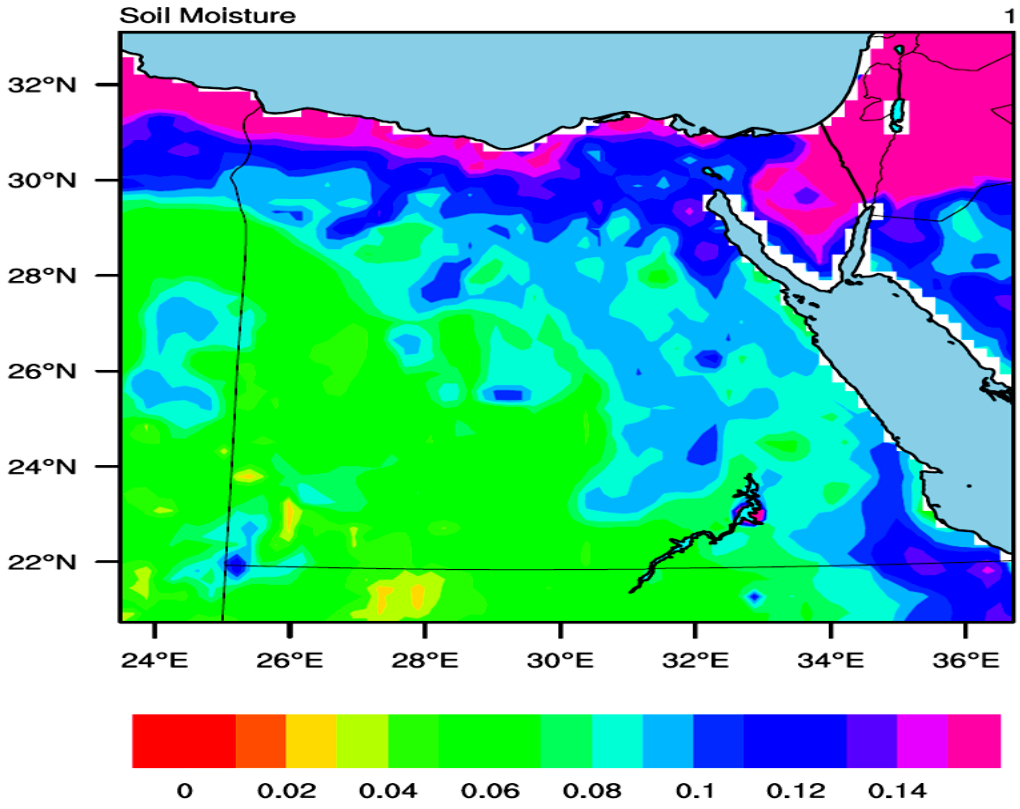

Figure 1. The figure shows the interpolated ESACCI satellite soil moisture product on the RegCM4 curvilinear grid.

2.2. Observational Data

To evaluate the RegCM4 model performance, various sources of datasets have been utilized:

1. Climate Research Unit (CRU; [22]): was used to evaluate the simulated TMX and TMN on a regional scale over the period 2001–2010. Basically, CRU is based on upscaling of the meteorological observations across the globe and then interpolates the meteorological variables over the land units on a grid of 0.5 × 0.5 degrees grid spacing. CRU was considered in the present study because it is available over a long period starting from 1901 till 2022. Additionally, CRU has no missed values over the selected domain as reported by [22]. For the purpose of the present study, CRU was bilinearly interpolated on the RegCM4 curvilinear grid following [11,31]. In this study, the last version (4.07) of the CRU was used.
2. Station observation (OBS): monthly average of the TMX and TMN were collected for fifteen stations representing different climate zones of Egypt over the period 2001–2010. Table 1 shows the station coordinates, world meteorological organization (WMO) ID and elevation above mean sea level (in meters). It should be noted that the climatology (of each month) was calculated to produce the climatological annual cycle of the TMX/TMN (to evaluate the RegCM4 performance at each location).

Table 1. The table shows station coordinates World Meteorological Organization (WMO) ID and elevation above mean sea level (in meters).

Station	WMO Code	Longitude (°E)	Latitude (°N)	Elevation (m)
Marsa-Matrouh	62306	27.22	31.33	25
Dabaa	62309	28.47	30.93	17
Alexandria	62318	29.95	31.18	-2.626
Port Said	62332	32.20	31.28	0.8
Arish	62337	33.49	31.09	30.57
Cairo	62366	31.40	30.13	64.12
Assyut	62393	31.02	27.05	226
Luxor	62405	32.70	25.67	83.64
Asswan	62414	32.78	23.97	192.53
Farafra	62423	27.97	27.05	77.79
Dakhla	62432	29.00	25.29	107.26
Ismailia	62440	32.23	30.59	10.14
Ras Sedr	62455	32.72	29.59	3.26
Hurgada	62463	33.82	27.18	7.79
Shallateen	62476	35.58	23.13	19.44

3. Results

3.1. Soil Moisture Initialization

To understand how the simulated TMX/TMN is sensitive to the initialized soil moisture (ESACCI relative to bare soil); a diagnostic analysis was conducted between the bare soil (NoMois) and ESACCI (Mois). The significant difference between Mois and NoMois was calculated for each grid point using Student *t*-test with α equals 5%. Figure 2 shows the simulated total albedo (AL), surface upward short wave radiation (RSUS), surface net short wave radiation (RSNS) and global incident solar radiation (RSDS). From Figure 2, it can be noted that switching between bare soil and ESACCI imposes a notable influence on the aforementioned variables. For instance, Mois has lower AL than NoMois over majority of the land units (by 10%) except for the Delta region and river Nile (where no change has been noticed; Figure 2a–c). As a result, Mois has lower RSUS (by 10–30 W m^{-2}) than NoMois (see Figure 2d–f).

Additionally, Mois has higher RSNS (by 10–30 W m^{-2}) than NoMois as indicated in Figure 2g–i. Therefore, it can be noted that switching between bare soil and ESACCI induces a warming effect (as will be investigated in the upcoming sections). This behavior was noted although the soil moisture in Egypt has values ranging between 0 and 0.15 (see Figure 1). This means that inclusion of the ESACCI (as an initial condition of the soil moisture) has a considerable effect in the arid regions (as in this study). Finally, Mois has higher RSDS (by ~5 W m^{-2}) than NoMois (Figure 2j–l). This means that switching between NoMois and Mois has no considerable effect on the simulated RSDS and therefore the PET as reported by [26]. Besides the noted effect on the radiation variables, the influence of the soil moisture initialization extends to include the planetary boundary layer height (PBL) and sensible heat flux (SHF).

From Figure 3, it can be observed that Mois has higher PBL (by 30–110 m) than NoMois (see Figure 3a–c). Such behavior can be attributed to the fact that RSNS increases by switching from bare soil to initialization from the ESACCI satellite based product. As a result, the Mois has increased the SHF (by 15–40 W m^{-2}) relative to the NoMois. In Figure 4, the influence of the soil moisture initialization on the near surface relative humidity (RH), TMX and TMN was discussed. From Figure 4, it can be noticed that the Mois decreases the RH (by 10–30%) compared to the NoMois (Figure 4a–c). Such behavior can be explained by the fact that Mois shows higher RSNS (see Figure 2g–i) more than the NoMois. As a result, the Mois disperses the water vapor more than the NoMois.

Concerning the TMX, Mois is warmer than NoMois (by 1–3°C; Figure 4d–f) which can attributed to two reasons: 1—Mois has higher RSNS than NoMois and 2—Mois has lower RH than NoMois. For the TMN, Mois is warmer than NoMois particularly in the region of 22–24°N (by 1–6°C; Figure 4g–i). From Figure 4, it can be also noted that switching from bare soil to ESACCI satellite product induces a considerable effect on TMN more than TMX.

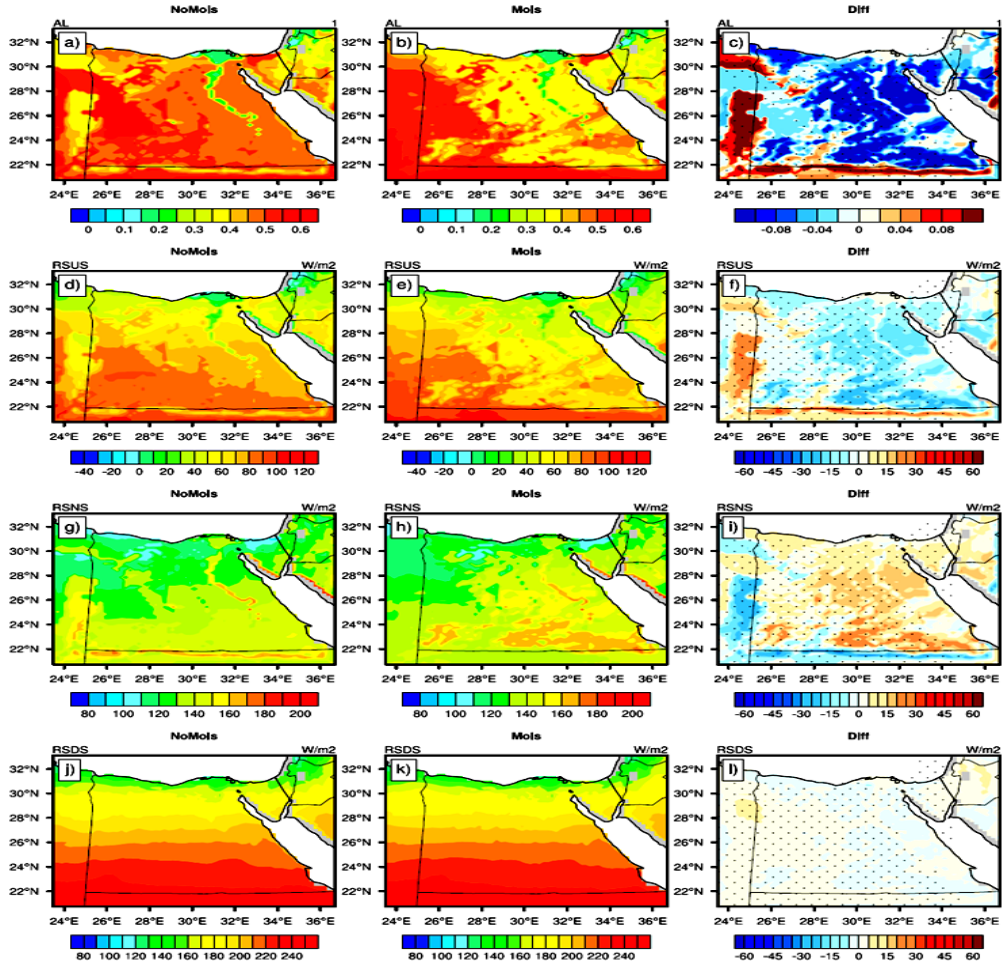

Figure 2. The figure shows the comparison between NoMois and Mois for the variables: 1—total albedo (Al; (**a**–**c**)), 2—surface upward short wave radiation (RSUS; (**d**–**f**)), 3—surface net short wave radiation (RSNS; (**g**–**i**)) and 4—downward short wave radiation (RSDS; (**j**–**l**)).

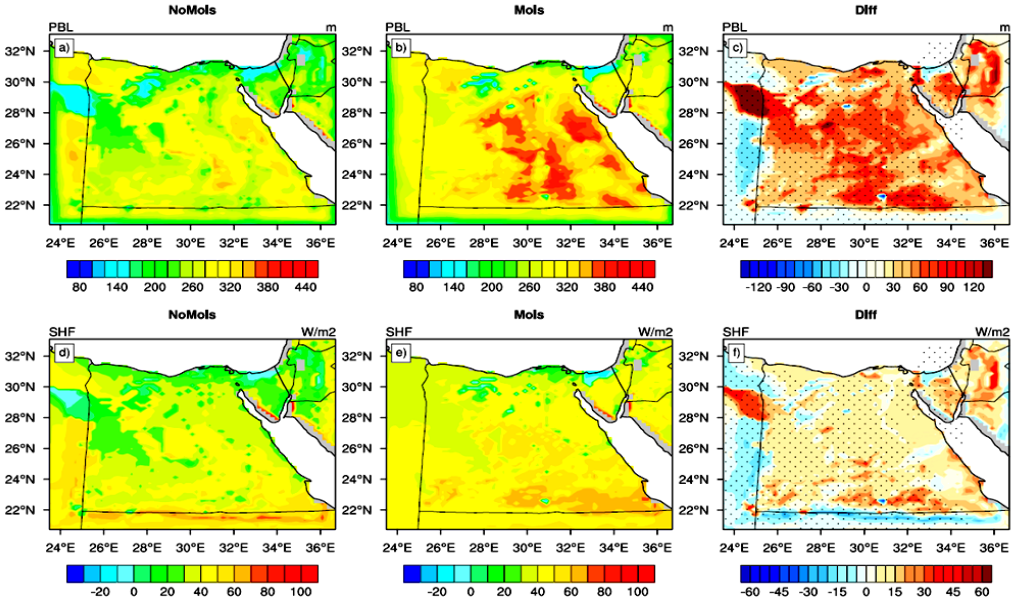

Figure 3. The figure shows the comparison between NoMois and Mois for the variables: 1—planetary boundary layer height (PBL; (**a**–**c**)) and 2—surface sensible heat flux. (SHF; (**d**–**f**)).

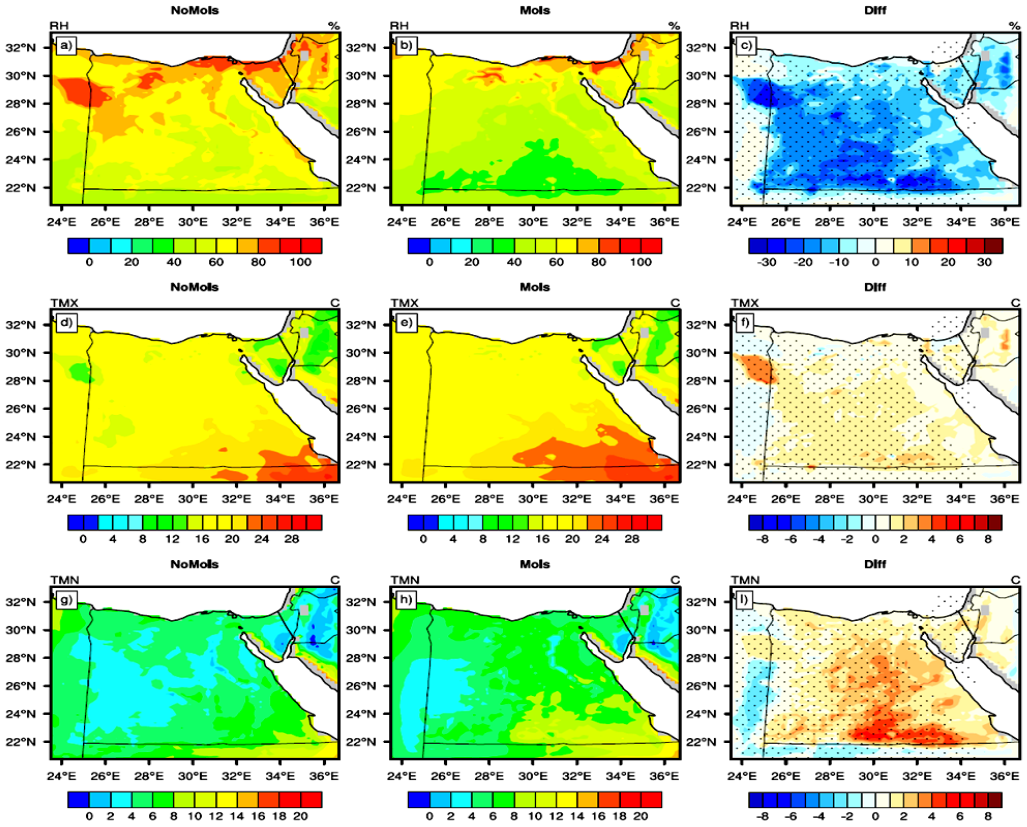

Figure 4. The figure shows the comparison between NoMois and Mois for the variables: 1—near surface relative humidity (RH; (**a**–**c**)), 2—near surface maximum air temperature (TMX; (**d**–**f**)) and 3—near surface minimum air temperature (TMN; (**g**–**i**)).

3.2. Land Surface Parameterization

3.2.1. Diagnostic Analysis

To understand how the land surface parameterization (BATS/CLM45) can affect the simulated TMX/TMN, a diagnostic analysis has been first performed for the following variables: ground temperature (TS), sensible heat flux (SHF), planetary boundary layer height (PBL) and near surface relative humidity (RH). Figure 5 shows the comparison between the BATS and CLM45 concerning the aforementioned variables. The significant difference between BATS and CLM45 was calculated using Student *t*-test with α equals 5%. From Figure 5, it can be noted that CLM45 has lower TS than BATS (by 1–5°C; see Figure 5a–c). Because TS controls the heat transferred from the ground to the adjacent layer of the atmosphere, the SHF is affected too. As a result, the CLM45 has lower SHF (by 10–40 W m^{-2}) than the BATS (Figure 5d–f).

Concerning the PBL, it can be observed that the CLM45 has shallower PBL than the BATS (up to 120 m; Figure 5g–i). Finally, the CLM45 has lower RH (up to 30%) than the BATS particularly in the region of 26–32°N. On the other hand, the CLM45 has lower RH (by 5–10%) than the BATS in the region of 22–26°N (see Figure 5j–l). This noted behavior can be attributed to the fact that the CLM45 generates lower soil moisture than the BATS in agreements with the results reported by [14]. Additionally, the CLM45 has higher albedo (by 10%) than the BATS; while there was no noted change in the total cloud cover (Figure S1). Regarding the solar radiation budget, there was no significant change in the global incident solar radiation (RSDS). On the other hand, the CLM45 has lower (higher) upward short wave radiation RSUS (RSNS) than the BATS (see Figure S2). Such behavior can explain the observed cold bias of TMX/TMN as will discussed in Section 3.2.2. In Sections 3.1 and 3.2.1, it can be noted that soil moisture initialization has opposite effects compared to the one induced by the land surface parameterization. For instance,

switching between the bare soil and ESACCI induces an increase in the soil moisture. On the other hand, the CLM45 generate lower soil moisture than the BATS.

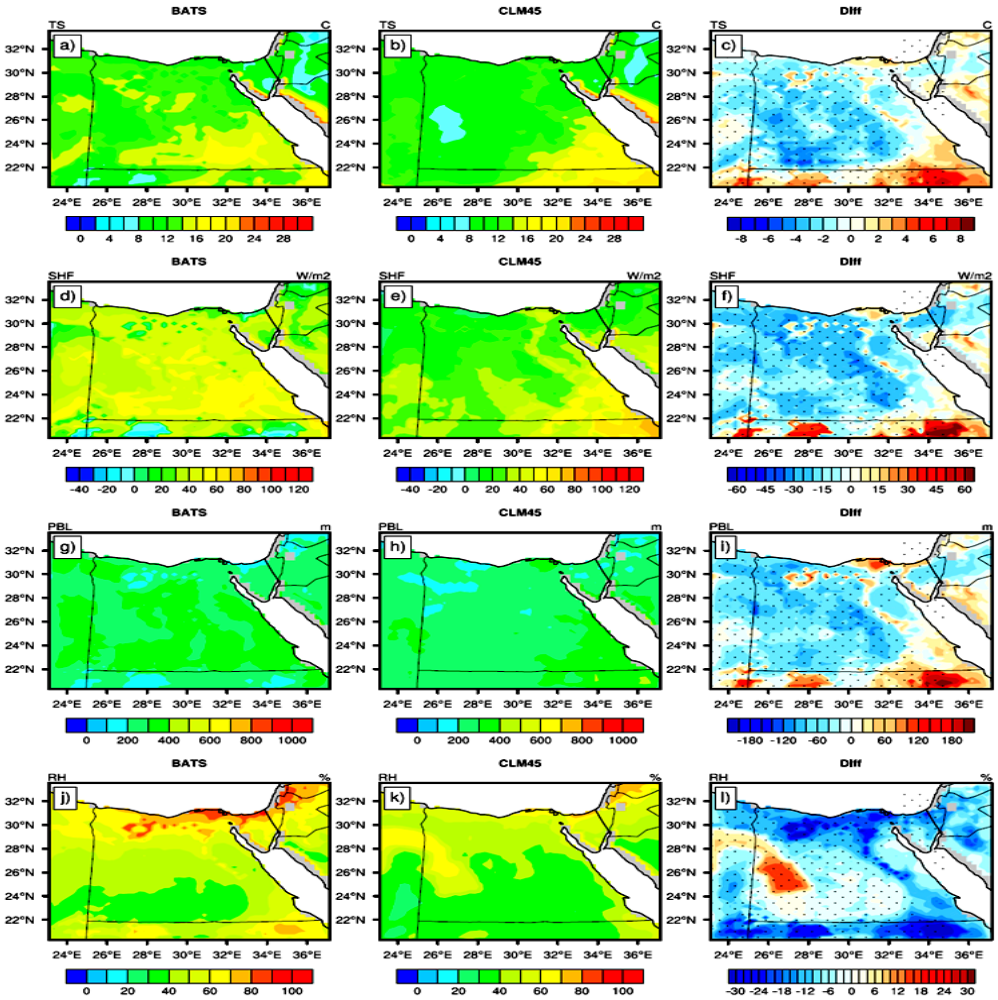

Figure 5. The figure shows the comparison between BATS and CLM45 land surface schemes for the variables: 1—ground temperature (TS; (**a**–**c**)), 2—sensible heat flux (SHF; (**d**–**f**)), 3—planetary boundary layer height (PBL; (**g**–**i**)) and 4—near surface relative humidity (RH; (**j**–**l**)).

3.2.2. The Influence on Maximum/Minimum Air Temperature (TMX/TMN)

Figure 6 shows the simulated TMX (by BATS/CLM45) with respect to the CRU for the seasons: spring (March-April-May; MAM), summer (June-July-August; JJA), autumn (September-October-November; SON) and winter (December-January-February; DJF). From Figure 6, it can be noted that the RegCM4 is able to reproduce the spatial pattern of the simulated TMX compared to the CRU in all seasons (Figure 6a–c, g–i, m–o, s–u). For instance, the TMX approaches its maximum values in the JJA followed by the SON, MAM and finally approaches its minimum values in the DJF. Additionally, it can be noted that the BATS induces an obvious warming effect particularly in the coasts of the Mediterranean and Red Sea. Such behavior can be observed in the MAM, JJA and SON (see Figure 6d, j, p) where the bias ranges between 3 and 7°C. In the DJF, the situation is different (Figure 6v) because the warm bias approaches 2°C.

Switching from BATS to CLM45 induces a notable impact on the simulated TMX in all seasons. For example, the CLM45 induces a cooling effect which can be obviously seen in the coasts of the Mediterranean and Red Sea in all seasons (where the bias ranges between 2 and 4°C; see Figure 6e, k, q, w). Additionally, the noted warm bias (induced by the BATS) has been replaced with a cold bias of 1–3°C. Such behavior can be explained by

the significant difference between the CLM45 and BATS. For instance, it can be observed that CLM45 is cooler than BATS by 2–5°C (Figure 6f, l, r, x).

Like TMX, the RegCM4 is able to capture the spatial pattern of the simulated TMN in all seasons with respect to the CRU (Figure 7a–c, g–i, m–o, s–u). Furthermore, BATS shows a warm bias of 1–6°C in the MAM, JJA and SON (Figure 7d,j,p) and 1–6°C in the DJF (Figure 7v). For the CLM45, the situation is quite different because there is a warm bias of 1–3°C observed mainly in the Delta region, a cold bias (with the same order of magnitude in the MAM, JJA and SON (Figure 7e, k, q) and −2 to +1°C in the DJF (Figure 7w). Qualitatively, it can be observed that CLM45 is cooler than BATS (by 2–5°C) and warmer than BATS in the northern and eastern coasts of Egypt (by 1–4°C; see Figure 7f, l, r, x). Bottom-line, the BATS promotes a net warming effect, while the CLM45 induces a net cooling effect concerning the simulated TMX/TMN.

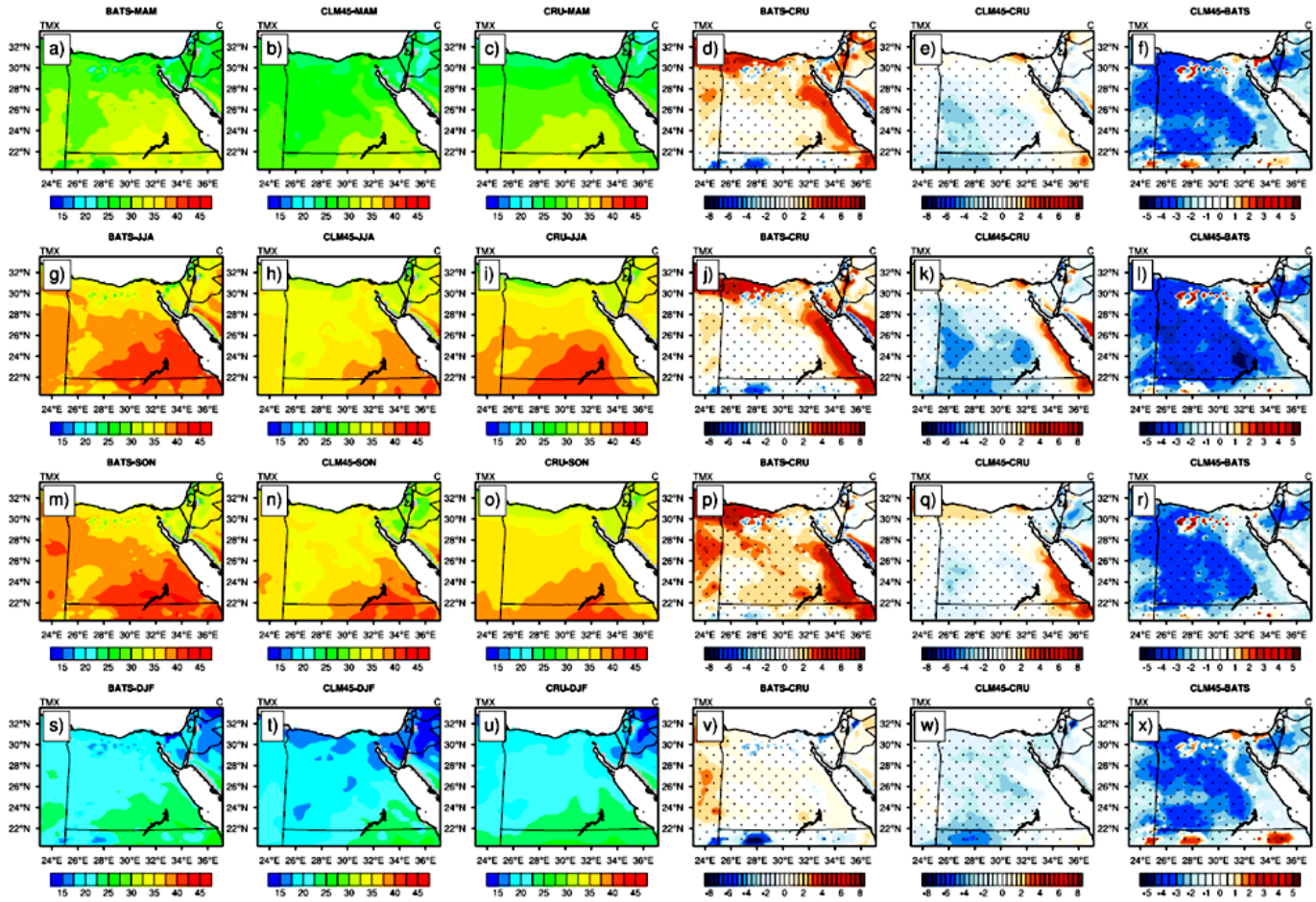

Figure 6. The figure shows the simulated daily maximum air temperature over the period 2001–2010 (TMX; in °C) for the seasons: MAM in the first row (**a**–**f**); JJA in the second (**g**–**l**); SON in the third (**m**–**r**), DJF in the fourth (**s**–**x**). For each row, BATS is on the left, followed by CLM45. CRU is in the third from left, BATS minus CRU, CLM45 minus CRU and the difference between CLM45 and BATS. Significant difference/bias is indicated in black dots using student *t*-test with alpha equals 5%.

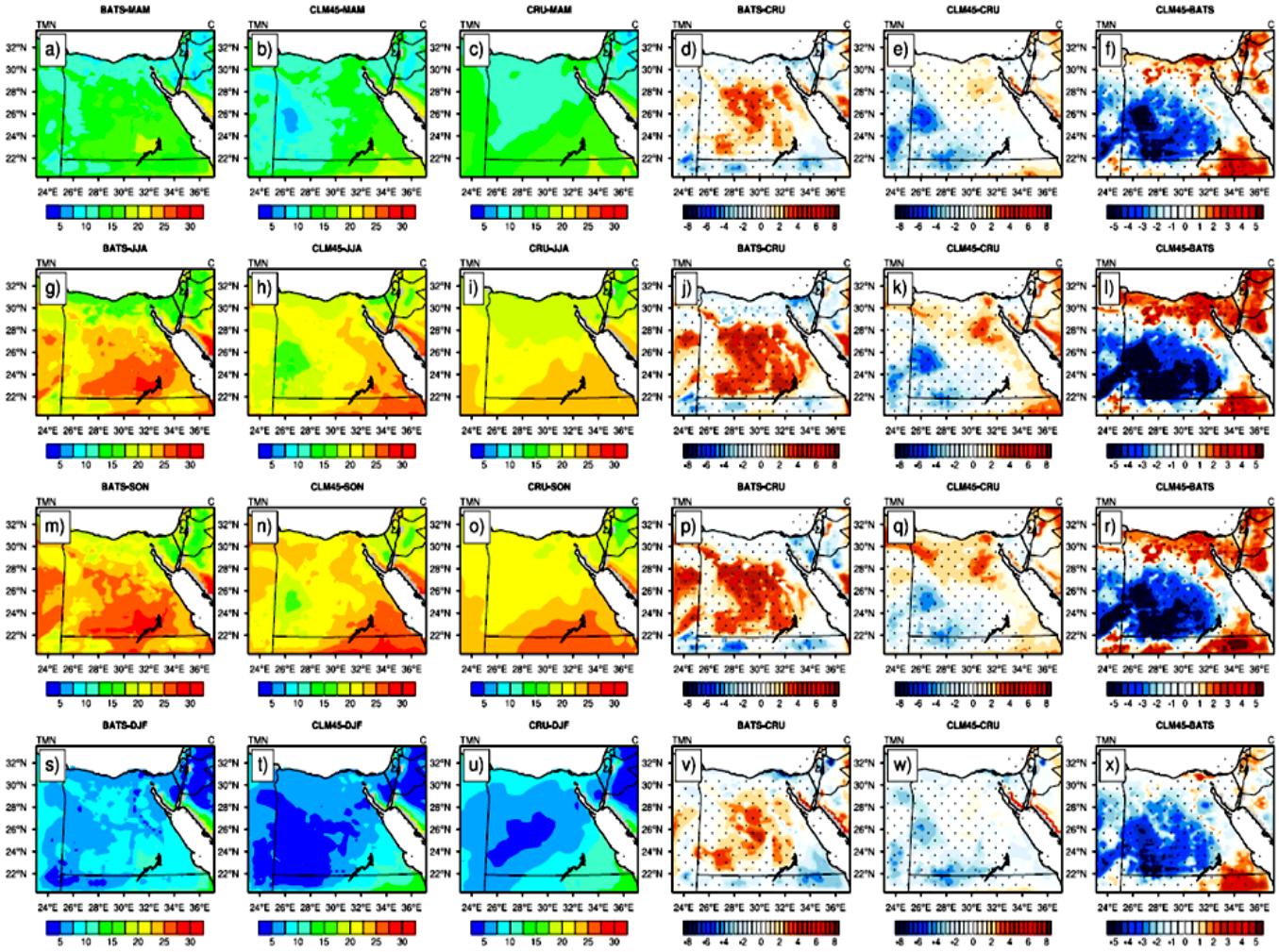

Figure 7. The figure shows the simulated daily minimum air temperature over the period 2001–2010 (TMN; in °C) for the seasons: MAM in the first row (**a**–**f**); JJA in the second (**g**–**l**); SON in the third (**m**–**r**), DJF in the fourth (**s**–**x**). For each row, BATS is on the left, followed by CLM45. CRU is in the third from left, BATS minus CRU, CLM45 minus CRU and the difference between CLM45 and BATS. Significant difference/bias is indicated in black dots using student *t*-test with alpha equals 5%.

3.3. Climatological Annual Cycle

In this section, behavior of the BATS/CLM45 is examined concerning the climatological annual cycle (for the fifteen locations reported in Table 1) with respect to the station observations (OBS).

3.3.1. Maximum Air Temperature (TMX)

Figure 8 shows the climatological annual cycle of the simulated TMX compared to the OBS. From Figure 8, it can be noted that BATS/CLM45 can reproduce the annual cycle of the TMX with respect to the OBS; however the behavior of the BATS/CLM45 varies with the location and month. For instance, the BATS is close to the OBS in February and October in Alexandria. On the other hand, the CLM45 is close to the OBS in January, November and December. Additionally, both schemes overestimate the TMX during rest of months. The same behavior can be observed in Arish because the BATS is close to the OBS in the months January to March and October to December, while the CLM45 is close to the OBS during rest of months.

Concerning Asswan, Assyut, Dakhla, Farafra, Luxor and Ras-Sedr; BATS is close to the OBS while CLM45 underestimates the TMX in comparison with the OBS. In Cairo, Dabaa, Ismailia, Marsa-Matrouh and Port-Said, it can be observed that both BATS and CLM45 underestimate the TMX compared to the OBS, yet CLM45 is closer to the OBS than BATS. Finally in Shallateen, the situation is different since there is no difference between BATS and CLM45 (in all months) with respect to the OBS.

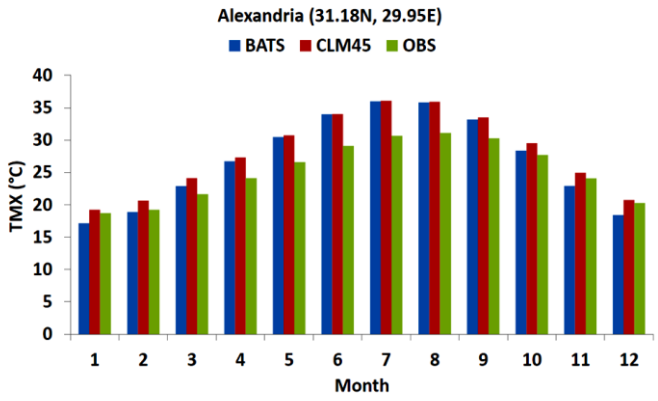

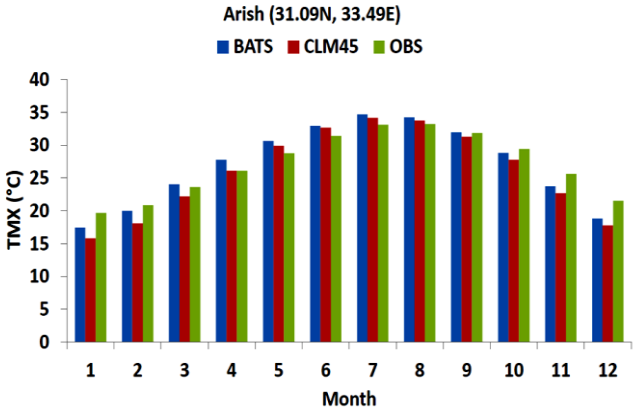

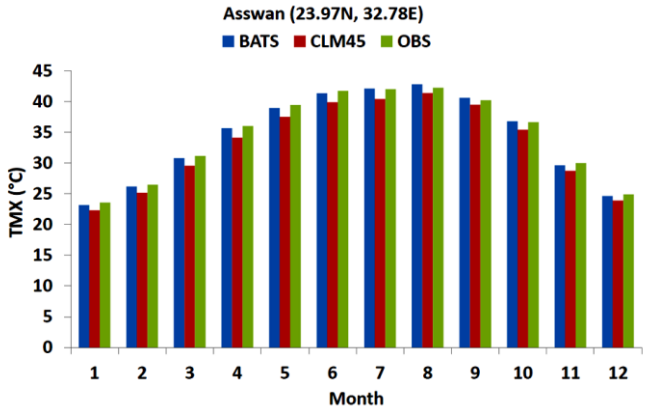

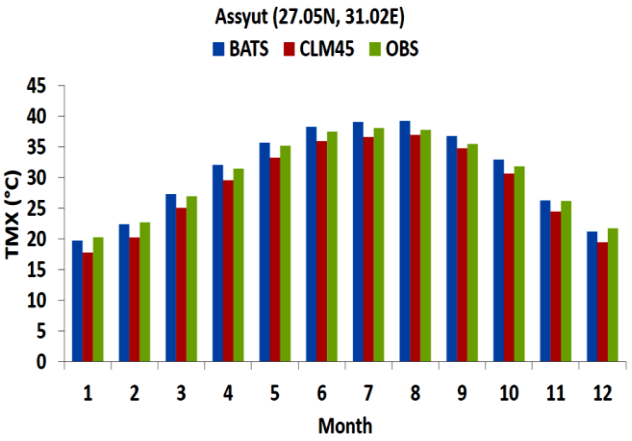

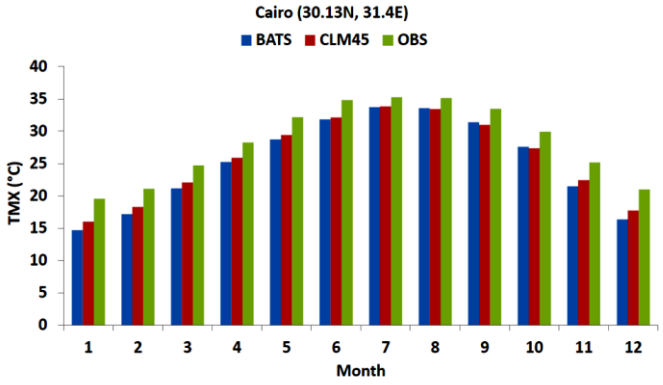

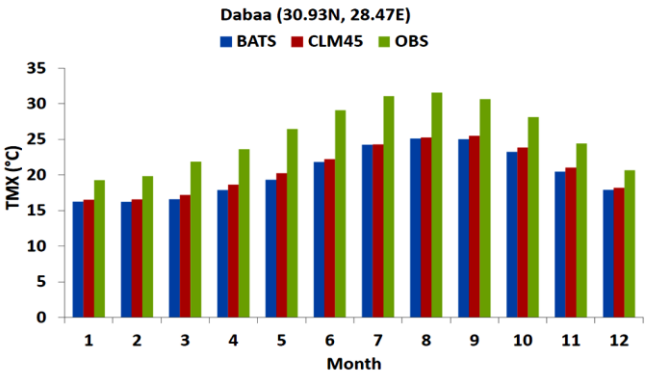

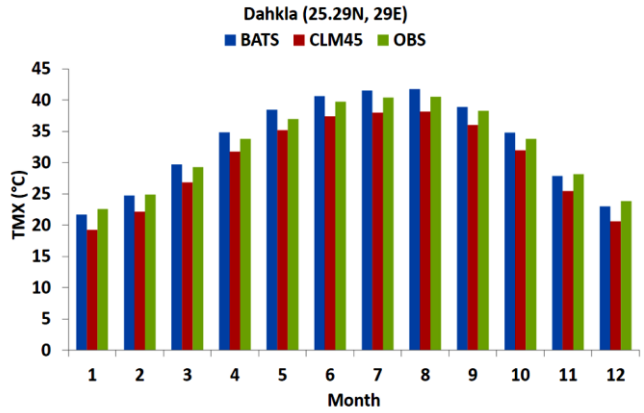
Dahkla (25.29N, 29E)
BATS CLM45 OBS
TMX (°C)
Month

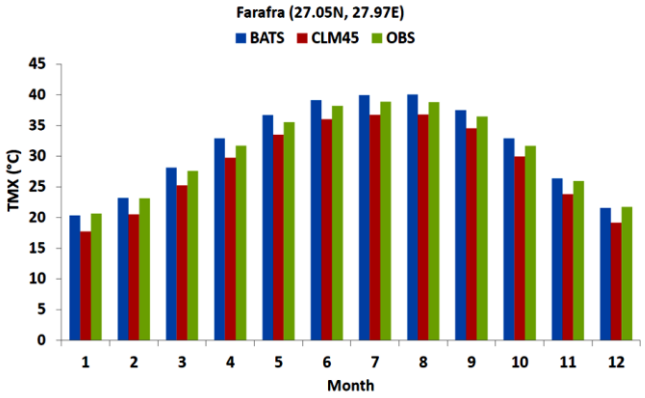
Farafra (27.05N, 27.97E)
BATS CLM45 OBS
TMX (°C)
Month

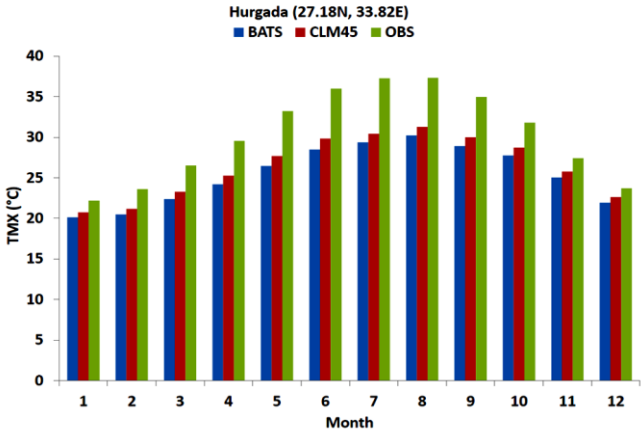
Hurgada (27.18N, 33.82E)
BATS CLM45 OBS
TMX (°C)
Month

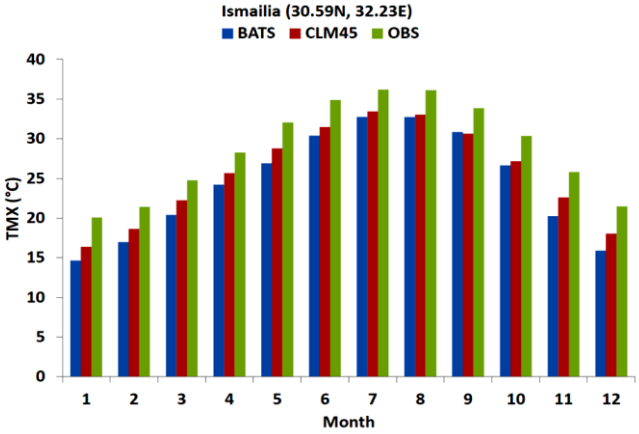
Ismailia (30.59N, 32.23E)
BATS CLM45 OBS
TMX (°C)
Month

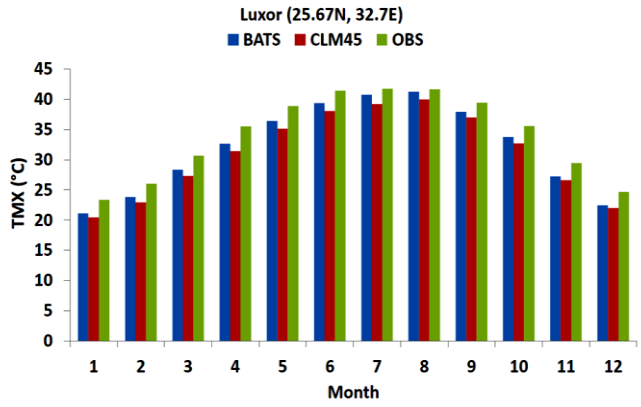
Luxor (25.67N, 32.7E)
BATS CLM45 OBS
TMX (°C)
Month

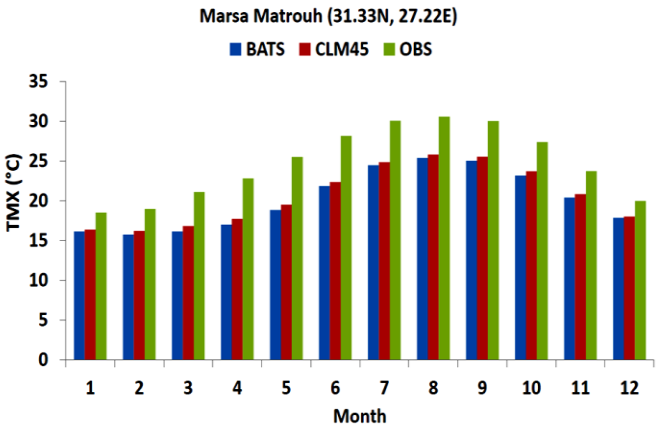
Marsa Matrouh (31.33N, 27.22E)
BATS CLM45 OBS
TMX (°C)
Month

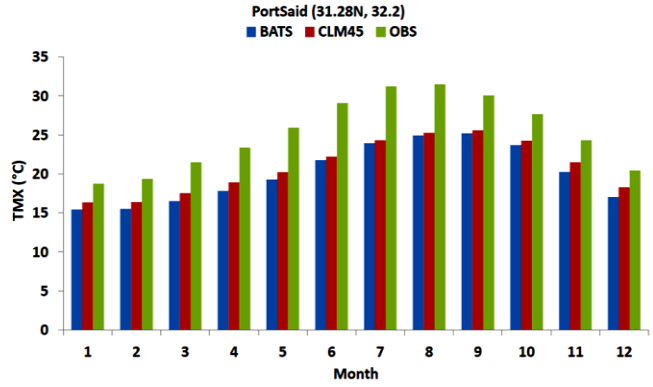
PortSaid (31.28N, 32.2)
BATS CLM45 OBS
TMX (°C)
Month

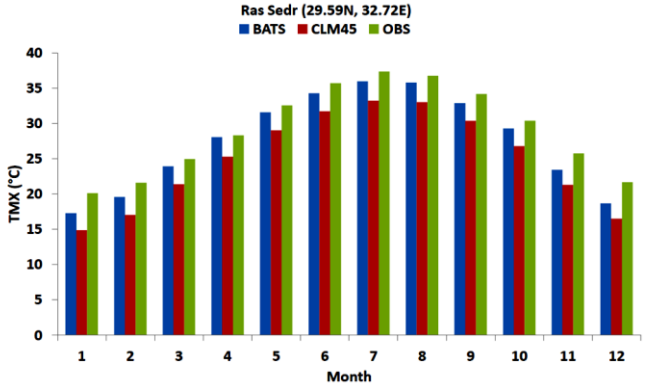
Ras Sedr (29.59N, 32.72E)
BATS CLM45 OBS
TMX (°C)
Month

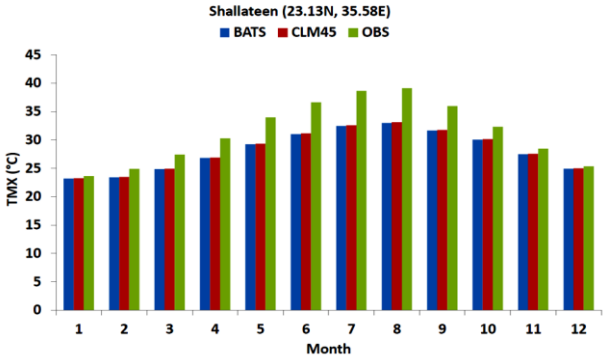

Figure 8. The figure shows the climatological annual cycle of the daily maximum air temperature over the period 2001–2010 (TMX; in °C) for the fifteen locations indicated in Table 1. BATS scheme is indicated in blue color, CLM45 scheme in red color and station observation (OBS) in green color.

3.3.2. Minimum Air Temperature (TMN)

Like TMX, the BATS/CLM45 is able to simulate the climatological annual cycle of the TMN with respect to the OBS (Figure 9). However, behavior of the BATS/CLM45 is different from the one noted in Section 3.3.1. For instance, in majority of locations the CLM45 is closer to the OBS than the BATS despite of the observed over/underestimation of the simulated TMN (compared to the OBS). Additionally in Luxor, the BATS outperforms the CLM45 in simulating the TMN. Also in Dabaa and Hurgada, there is no scheme performs better than the other one. Finally in Shallateen, there is no difference between the BATS and CLM45 in comparison with the OBS. The noted behavior of the simulated TMX/TMN (with respect to the OBS) can be attributed to the fact that the local geographic features of the fifteen locations are not present in the static data of the RegCM4 as reported by [29]. Additionally, behavior of the BATS/CLM45 has been quantified (with respect to the CRU for the fifteen locations) using the mean bias (MB) as a statistical metrics (see Table 2).

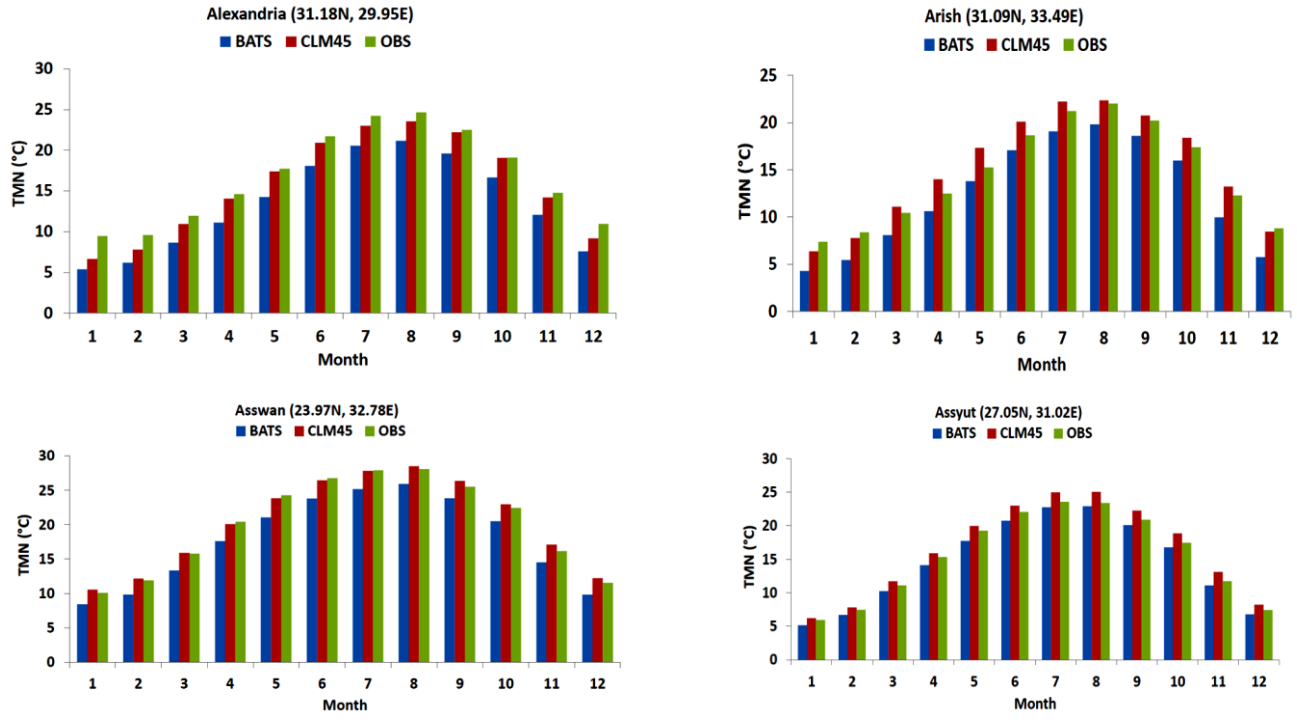

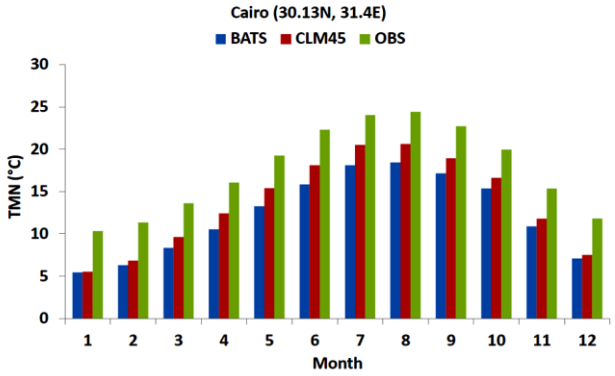
Cairo (30.13N, 31.4E)
BATS CLM45 OBS
TMN (°C)
Month

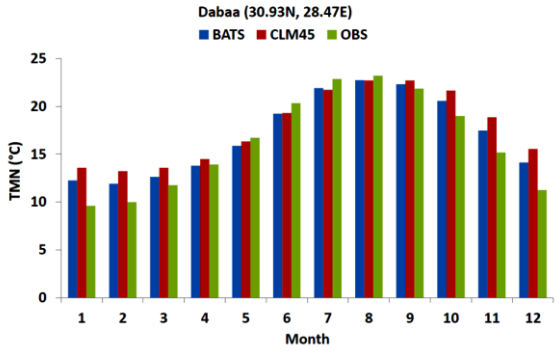
Dabaa (30.93N, 28.47E)
BATS CLM45 OBS
TMN (°C)
Month

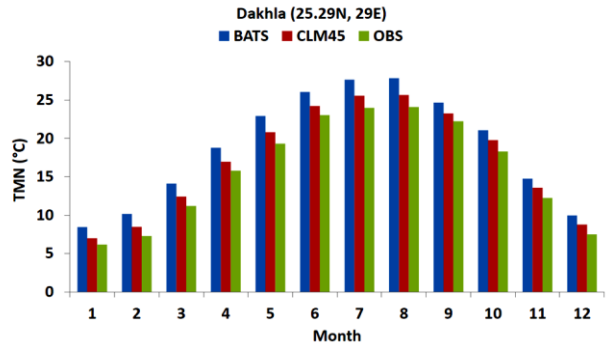
Dakhla (25.29N, 29E)
BATS CLM45 OBS
TMN (°C)
Month

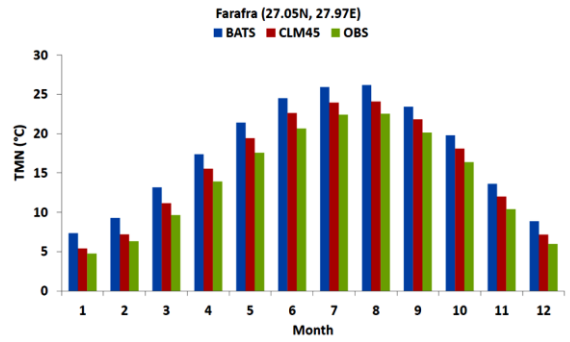
Farafra (27.05N, 27.97E)
BATS CLM45 OBS
TMN (°C)
Month

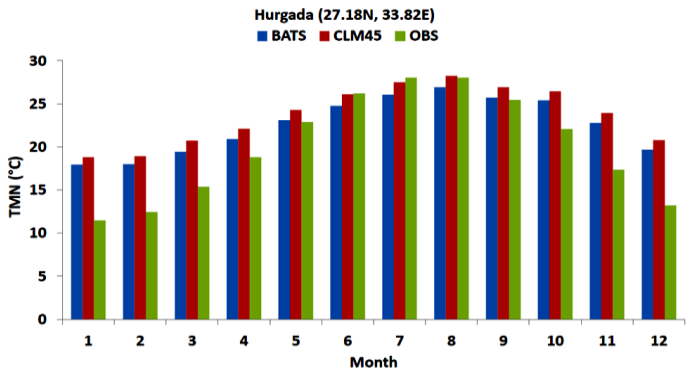
Hurgada (27.18N, 33.82E)
BATS CLM45 OBS
TMN (°C)
Month

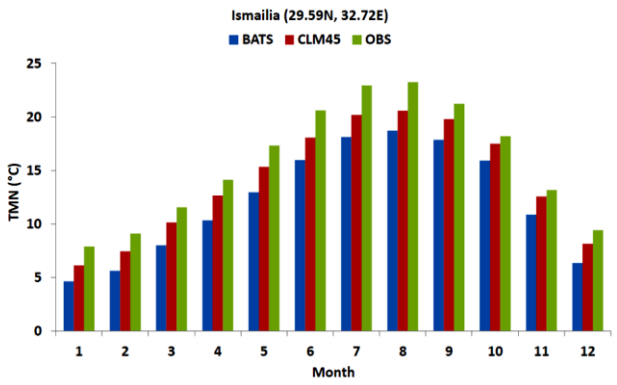
Ismailia (29.59N, 32.72E)
BATS CLM45 OBS
TMN (°C)
Month

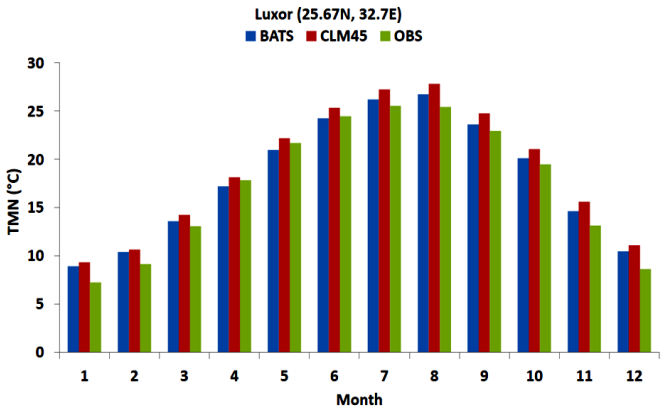
Luxor (25.67N, 32.7E)
BATS CLM45 OBS
TMN (°C)
Month

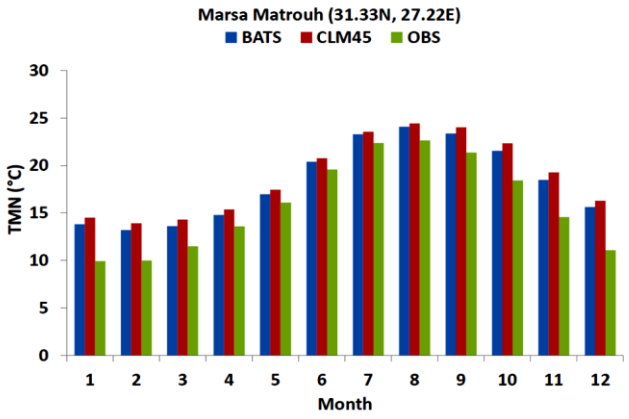
Marsa Matrouh (31.33N, 27.22E)
BATS CLM45 OBS
TMN (°C)
Month

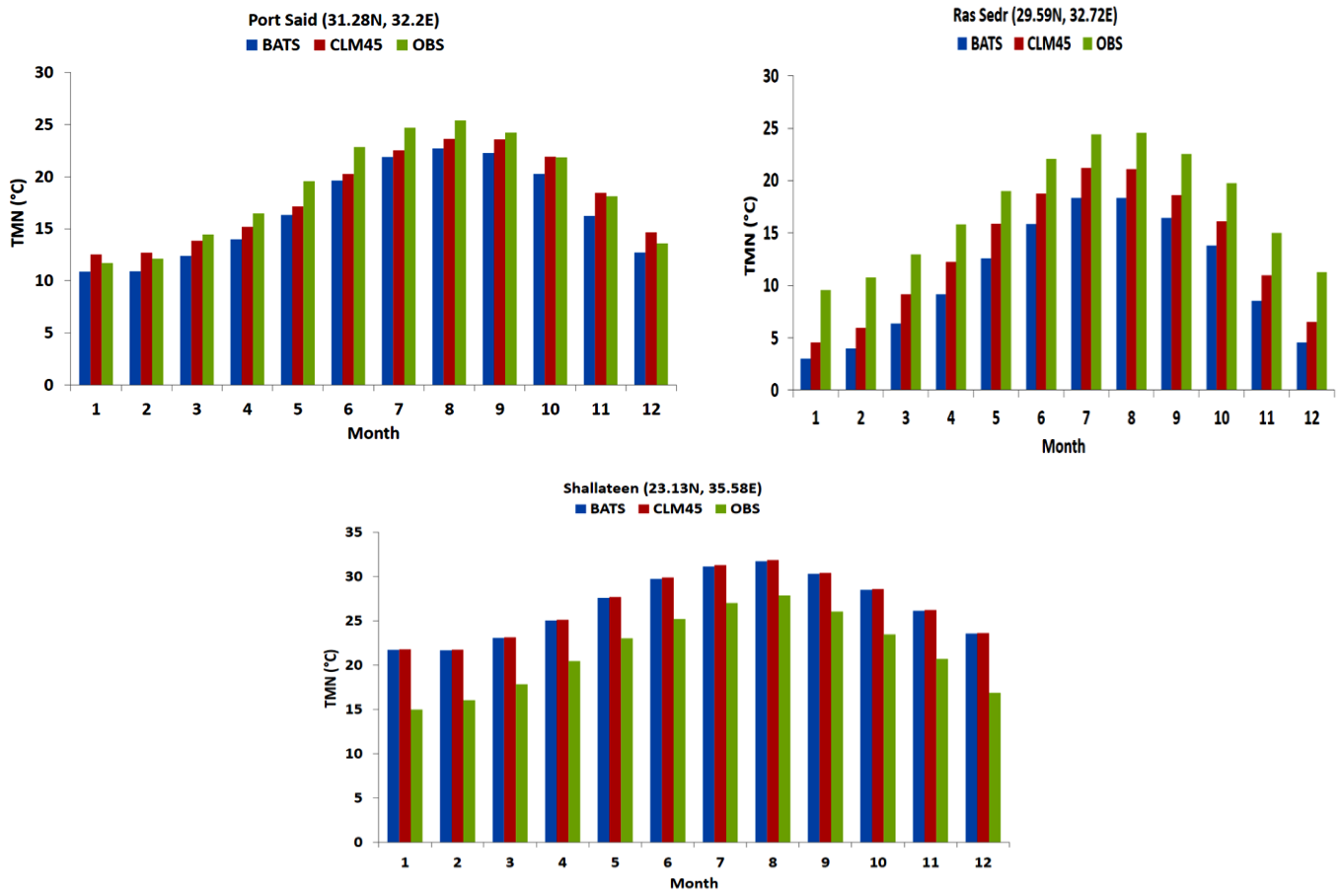

Figure 9. The figure shows the climatological annual cycle of the daily minimum air temperature over the period 2001–2010 (TMN; in °C) for the fifteen locations indicated in Table 1. BATS scheme is indicated in blue color, CLM45 scheme in red color and station observation (OBS) in green color.

Table 2. The table shows the mean bias (MB; in °C) for the BATS/CLM45 concerning the simulated TMX/TMN for the fifteen locations indicated in Table 1.

Station	TMX		TMN	
	BATS	CLM45	BATS	CLM45
Marsa-Matrouh	−4.56	−4.08	2.33	2.92
Dabaa	−5.20	−4.76	0.76	1.50
Alexandria	1.77	2.76	−3.32	−1.02
Port Said	−5.15	−4.36	−2.07	−0.72
Arish	−0.01	−1.08	−2.16	0.62
Cairo	−3.13	−2.57	−5.36	−3.94
Assyut	0.47	−1.70	−0.87	0.94
Luxor	−1.93	−2.97	0.71	1.57
Asswan	−0.14	−1.37	−2.24	0.25
Farafra	0.70	−2.21	3.35	1.48
Dakhla	0.48	−2.45	2.93	1.27
Ismailia	−4.38	−3.09	−3.61	−1.68
Ras Sedr	−1.55	−4.07	−6.39	−3.89
Hurgada	−4.84	−3.89	2.43	3.61
Shallateen	−3.21	−3.12	5.06	5.15

4. Discussion and Conclusions

Soil moisture is important variable in the global terrestrial hydrology cycle and it controls the surface regional climate by perturbing the total evapotranspiration budget and surface energy balance. Such effects have been investigated in various regions across the global using the RegCM4 regional climate model [7–9]. Additionally, the influence of soil moisture on the global incident solar radiation [10], simulated terrestrial carbon fluxes [11, 12] and potential evapotranspiration [13] has been also examined within the framework of the RegCM4. However, the indicated effects of the soil moisture have been studied in wet regions. In arid regions (e.g., Egypt), such effects have not been examined till the present day. Additionally, the sensitivity of TMX/TMN of Egypt to the land surface parameterization (considering the initialization with a global satellite soil moisture product) has not been also investigated.

In the present study, the RegCM4 regional climate model was used to address the sensitivity of the simulated TMX/TMN of Egypt to different initial conditions of the soil moisture (bare soil against the ESACCI satellite soil moisture product). Additionally, the role of the land surface parameterization (BATS/CLM45) in simulating the TMX/TMN was also examined with respect to the CRU and station observations. To achieve this task, four 13-year simulations were conducted (1998-2010). In each simulation, the first three years were not considered in the analysis for the soil moisture to approach an equilibrium state following [9, 13, 14].

The results showed that switching from the bare soil to the ESACCI satellite product induces a considerable influence on the simulated TMX/TMN through changes in the total albedo, solar radiation budget, planetary boundary layer height, sensible heat flux and near surface relative humidity. Additionally, switching from BATS to CLM45 led to decrease of the ground temperature, sensible heat flux, and planetary boundary layer height and near surface relative humidity. As a result, heat flow (from the earth surface to the adjacent atmosphere layer and eventually to the whole planetary boundary layer) decreased. Such behavior can explain the warm (cold) bias of the BATS (CLM45) with respect to the CRU. Despite of the noted biases, the CLM45 succeeded in reducing the observed warm bias of the BATS. Compared to the OBS, behavior of the BATS/CLM45 varies with the location of interest concerning the TMX. For the TMN, the CLM45 outperforms the BATS in majority of locations (see Figure 9).

It is important to observe that the global incident solar radiation is insensitive either to the soil moisture status or the land surface parameterization (Figures 2 and S2). Such behavior suggests that RSDS is the main driver controlling the PET followed by the daily mean air temperature [26,32]. In conclusion, the RegCM4 regional climate model can be recommended for future studies concerning the seasonal prediction/climate change of the daily TMX/TMN and temperature indices of Egypt (under different warming scenarios) when it is configured with the CLM45 land surface model and initialized with the ESACCI satellite product.

In comparison with the OBS, caution must be taken in selecting the suitable scheme in the location of study. Given the observed effects (by switching from bare soil to ESACCI satellite product and land surface parameterization), it is recommended to investigate such effects in other arid regions (e.g., Arabian peninsula) to ensure an optimized performance of the RegCM4 with respect to reanalysis products and station observations. In a future work, the following points need to be addressed:

1. Running the RegCM in a convective permitting mode and parameterized convective schemes following [25].
2. Revising the results reported by [33, 34] when the RegCM4 is configured with the CLM45 land surface model and initialized with the ESACCI product.
3. Assessing the diurnal and daily variations of the RegCM4-CLM45 regional coupled climate model with the results reported by [35].

Because of the notable influence of the ESACCI (relative to the bare soil) and the difference between the BATS and CLM45 concerning the simulated TMX/TMN, it is suggested to examine the influence of ESACCI in various applications such as soil temperature profile [36], extreme storms [37], atmospheric chemistry (e.g., surface ozone; [38]) and potential evapotranspiration [39]. Additionally, the influence of land-surface hydrology schemes [3, 40] on the surface climate of the MENA region will be also investigated.

Supplementary Materials: The following supporting information can be downloaded at: www.mdpi.com/xxx/s1, www.mdpi.com/xxx/s2. Figure S1: The figure shows the total albedo and total cloud cover. Figure S2: The figure shows the solar radiation budget.

Author Contributions: Conceptualization, S.A.A.; methodology, S.A.A.; software, S.A.A.; validation, S.A.A. and S.M.M.; formal analysis, S.A.A.; investigation, S.A.A.; resources, S.A.A. and S.M.M.; data curation, S.A.A. and S.M.M.; writing—original draft preparation, S.A.A.; writing—review and editing, S.A.A.; visualization, S.A.A. and S.M.M.; supervision, S.A.A.; project administration, S.A.A. All authors have read and agreed to the published version of the manuscript.

Funding: No funding was received for this study.

Institutional Review Board Statement: Not applicable.

Data Availability Statement: Not applicable.

Informed Consent Statement: Not applicable.

Acknowledgments: Egyptian Meteorological Authority (EMA) is acknowledged for providing the computational power to conduct the RegCM4 simulations and station observations to evaluate the RegCM4 performance in different locations concerning the climatological annual cycle. University of East Anglia is acknowledged for providing the Climate Research Unit of the monthly average daily maximum and minimum air temperature from the web link https://crudata.uea.ac.uk/cru/data/hrg/cru_ts_4.07/cruts.2304141047.v4.07/ (accessed on 20 June 2023).

Conflicts of Interest: There is no conflict of interest.

References

1. Fisher, B.J.; Huntzinger, N.D.; Schwalm, C.R.; Sitch, S. Modelling the terrestrial biosphere. *Ann. Rev. Environ. Resour.* **2014**, *39*, 91–123.
2. Stuart, F.C., III; Matson, P.A.; Mooney, H.A. *Principles of Terrestrial Ecosystem Ecology*; QH541.C3595 ©; Spinger: New York, NY, USA, 2002; pp. 4–211.
3. Anwar, S.A.; Zakey, A.; Robaa, S.; Wahab, M.M.A. The influence of two land-surface hydrology schemes on the regional climate of Africa using the RegCM4 model. *Theor. Appl. Clim.* **2019**, *136*, 1535–1548. https://doi.org/10.1007/s00704-018-2556-8.
4. Anwar, S.A. On the contribution of dynamic leaf area index in simulating the African climate using a regional climate model (RegCM4). *Theor. Appl. Clim.* **2019**, *138*, 1219–1230. https://doi.org/10.1007/s00704-019-02885-x.
5. Giorgi, F.; Coppola, E.; Solmon, F.; Mariotti, L.; Sylla, M.B.; Bi, X.; Elguindi, N.; Diro, G.T.; Nair, V.; Giuliani, G.; et al. RegCM4: Model description and preliminary tests over multiple CORDEX domains. *Clim. Res.* **2012**, *52*, 7–29. https://doi.org/10.3354/cr01018.
6. Oleson, K.W.; Lawrence, D.M.; Bonan, G.B.; Drewniak, B.; Huang, M.; Koven, C.D.; Levis, S.; Li, F.; Riley, W.J.; Subin, Z.M. et al. *Technical Description of Version 4.5 of the Community Land Model (CLM)*; NCAR Technical Note NCAR/TN-503þ STR; National Center for Atmospheric Research: Boulder, CO, USA, 2013.
7. Wang, X.; Chen, D.; Pang, G.; Anwar, S.A.; Ou, T.; Yang, M. Effects of cumulus parameterization and land-surface hydrology schemes on Tibetan Plateau climate simulation during the wet season: Insights from the RegCM4 model. *Clim. Dyn.* **2021**, *57*, 1853–1879. https://doi.org/10.1007/s00382-021-05781-1.
8. Anwar, S.A.; Reboita, M.S.; Llopart, M. On the sensitivity of the Amazon surface climate to two land-surface hydrology schemes using a high-resolution regional climate model (RegCM4). *Int. J. Clim.* **2022**, *42*, 2311–2327. https://doi.org/10.1002/joc.7367.
9. Anwar, S.A.; Srivastava, A.; Zerouali, B. On the role of land-surface hydrology schemes in simulating the daily maximum and minimum air temperatures of Australia using a regional climate model (RegCM4). *J. Water Clim. Chang.* **2023**, *14*, 989–1011. https://doi.org/10.2166/wcc.2023.512.

10. Anwar, S.A. Simulating the Surface Solar Irradiance of Africa Using a Regional Climate Model: Influence of Vegetation-Runoff Coupled System. *Eng. Proc.* **2023**, *31*, 15, https://doi.org/10.3390/ASEC2022-13814.
11. Anwar, S.A.; Diallo, I. A RCM investigation of the influence of vegetation status and runoff scheme on the summer gross primary production of Tropical Africa. *Theor. Appl. Clim.* **2021**, *145*, 1407–1420. https://doi.org/10.1007/s00704-021-03667-0.
12. Anwar, S.A.; Diallo, I. The influence of two land-surface hydrology schemes on the terrestrial carbon cycle of Africa: A regional climate model study. *Int. J. Clim.* **2021**, *41*, E1202–E1216. https://doi.org/10.1002/joc.6762.
13. Anwar, S.A.; Mamadou, O.; Diallo, I.; Sylla, M.B. On the Influence of Vegetation Cover Changes and Vegetation-Runoff Systems on the Simulated Summer Potential Evapotranspiration of Tropical Africa Using RegCM4. *Earth Syst. Environ.* **2021**, *5*, 883–897. https://doi.org/10.1007/s41748-021-00252-3.
14. Steiner, A.L.; Pal, J.S.; Rauscher, S.A.; Bell, J.L.; Diffenbaugh, N.S.; Boone, A.; Sloan, L.C.; Giorgi, F. Land surface coupling in regional climate simulations of the West African monsoon. *Clim. Dyn.* **2009**, *33*, 869–892. https://doi.org/10.1007/s00382-009-0543-6.
15. Oleson, K.W.; Niu, G.; Yang, Z.; Lawrence, D.M.; Thornton, P.E.; Lawrence, P.J.; Stöckli, R.; Dickinson, R.E.; Bonan, G.B.; Levis, S.; et al. Improvements to the Community Land Model and their impact on the hydrological cycle. *J. Geophys. Res.* **2008**, *113*, G01021. https://doi.org/10.1029/2007jg000563.
16. Dickinson, R.E.; Henderson-Sellers, A.; Kennedy, P.J. *Biosphere-Atmosphere Transfer Scheme (BATS) Version 1e as Coupled to the NCAR Community Climate Model (No. NCAR/TN-387þ STR*; University Corporation for Atmospheric Research: Boulder, CO, USA, 1993. https://doi.org/10.5065/D67W6959.
17. Maurya, R.K.S.; Sinha, P.; Mohanty, M.R.; Mohanty, U.C. Coupling of Community Land Model with RegCM4 for Indian Summer Monsoon Simulation. *Pure Appl. Geophys.* **2017**, *174*, 4251–4270. https://doi.org/10.1007/s00024-017-1641-8.
18. Chung, J.X.; Juneng, L.; Tangang, F.; Jamaluddin, A.F. Performances of BATS and CLM land-surface schemes in RegCM4 in simulating precipitation over CORDEX Southeast Asia domain. *Int. J. Clim.* **2018**, *38*, 794–810. https://doi.org/10.1002/joc.5211.
19. Constantinidou, K.; Hadjinicolaou, P.; Zittis, G.; Lelieveld, J. Sensitivity of simulated climate over the MENA region related to different land surface schemes in the WRF model. *Theor. Appl. Clim.* **2020**, *141*, 1431–1449. https://doi.org/10.1007/s00704-020-03258-5.
20. Dorigo, W.; Wagner, W.; Albergel, C.; Albrecht, F.; Balsamo, G.; Brocca, L.; Chung, D.; Ertl, M.; Forkel, M.; Gruber, A.; et al. ESA CCI Soil Moisture for improved Earth system understanding: State-of-the art and future directions. *Remote Sens. Environ.* **2017**, *203*, 185–215. https://doi.org/10.1016/j.rse.2017.07.001.
21. Gruber, A.; Scanlon, T.; van der Schalie, R.; Wagner, W.; Dorigo, W. Evolution of the ESA CCI Soil Moisture climate data records and their underlying merging methodology. *Earth Syst. Sci. Data* **2019**, *11*, 717–739. https://doi.org/10.5194/essd-11-717-2019.
22. Harris, I.; Osborn, T.J.; Jones, P.; Lister, D. Version 4 of the CRU TS monthly high-resolution gridded multivariate climate dataset. *Sci. Data* **2020**, *7*, 109; https://doi.org/10.1038/s41597-020-0453-3.
23. Pal, J.S.; Giorgi, F.; Bi, X.; Elguindi, N.; Solmon, F.; Gao, X.; Rauscher, S.A.; Francisco, R.; Zakey, A.; Winter, J.; et al. Regional Climate Modeling for the Developing World: The ICTP RegCM3 and RegCNET. *Bull. Am. Meteorol. Soc.* **2007**, *88*, 1395–1410. https://doi.org/10.1175/bams-88-9-1395.
24. Grell, G.A.; Dudhia, J.; Stauffer, D.R. *Description of the Fifth Generation Penn State/NCAR Mesoscale Model (MM5)*; NCAR Technical Note NCAR/TN-398+STR; Technical Note; National Center for Atmospheric Research (NCAR): Boulder, CO, USA, 1994; p.121. https://doi.org/10.5065/d60z716b.
25. Giorgi, F.; Coppola, E.; Giuliani, G.; Ciarlo`, J.M.; Pichelli, E.; Nogherotto, R.; Raffaele, F.; Malguzzi, P.; Davolio, S.; Stocchi, P.; et al. The Fifth Generation Regional Climate Modeling System, RegCM5: Description and Illustrative Examples at Parameterized Convection and Convection-Permitting Resolutions. *J. Geophys. Res. Atmos.* **2023**, *128*, e2022JD038199. https://doi.org/10.1029/2022jd038199.
26. Anwar, S.A.; Lazić, I. Estimating the Potential Evapotranspiration of Egypt Using a Regional Climate Model and a High-Resolution Reanalysis Dataset. *Environ. Sci. Proc.* **2023**, *25*, 29. https://doi.org/10.3390/ECWS-7-14253.
27. Anwar, S.A. Influence of Direct-Downscaling and One-Way Nesting on Daily Mean Air Temperature of Egypt Using the RegCM4. *J. Biomed. Res. Environ. Sci.* **2023**, *4*, 338–347. https://doi.org/10.37871/jbres1681.
28. Anwar, S.A.; Mostafa, S.M. On the Sensitivity of the Daily Mean Air Temperature of Egypt to Boundary Layer Schemes Using a High-Resolution Regional Climate Model (RegCM4). *J. Biomed. Res. Environ. Sci.* **2023**, *4*, 474–484. https://doi.org/10.37871/jbres1700.
29. Mostafa, S.M.; Anwar, S.A.; Zakey, A.S.; Wahab, M.M.A. Bias-Correcting the Maximum and Minimum Air Temperatures of Egypt Using a High-Resolution Regional Climate Model (RegCM4). *Eng. Proc.* **2023**, *31*, 73. https://doi.org/10.3390/ASEC2022-13852.
30. Kanamitsu, M.; Ebisuzaki, W.; Woollen, J.; Yang, S.K.; Hnilo, J.J.; Fiorino, M.; Potter, G.L. NCEP-DOE AMIP-II Reanalysis (R-2). *Bull. Am. Meteorol. Soc.* **2002**, *83*, 1631–1643.
31. Anwar, S.A.; Diallo, I. Modelling the Tropical African Climate using a state-of-the-art coupled regional climate-vegetation model. *Clim. Dyn.* **2022**, *58*, 97–113. https://doi.org/10.1007/s00382-021-05892-9.
32. Anwar, S.A.; Malcheva, K.; Srivastava, A. Estimating the potential evapotranspiration of Bulgaria using a high-resolution regional climate model. *Theor. Appl. Clim.* **2023**, *152*, 1175–1188. https://doi.org/10.1007/s00704-023-04438-9.

33. Anwar, S.A.; Salah, Z.; Khaled, W.; Zakey, A.S. Projecting the Potential Evapotranspiration in Egypt Using a High-Resolution Regional Climate Model (RegCM4). *Environ. Sci. Proc.* **2022**, *19*, 43. https://doi.org/10.3390/ecas2022-12841.
34. Ali, A.H.; Salah, Z.; Anwar, S.A.; Zakey, A.S. Influence of Agricultural Activity on the Surface Climate of New Delta of Egypt Using the RegCM4. *Eng. Proc.* **2023**, *31*, 43. https://doi.org/10.3390/ASEC2022-13763.
35. Frey, C.M.; Parlow, E.; Vogt, R.; Harhash, M.; Wahab, M.M.A. Flux measurements in Cairo. Part 1: In situ measurements and their applicability for comparison with satellite data. *Int. J. Clim.* **2011**, *31*, 218–231. https://doi.org/10.1002/joc.2140.
36. Anwar, S.A.; Hejabi, S. The Influence of Different Initial Conditions on the Soil Temperature Profile of Egypt Using a Regional Climate Model. *Eng. Proc.* **2023**, *31*, 62. https://doi.org/10.3390/ASEC2022-13850.
37. Mekawy, M.; Saber, M.; Mekhaimar, S.A.; Zakey, A.S.; Robaa, S.M.; Wahab, M.A. Evaluation of WRF Microphysics Schemes Performance Forced by Reanalysis and Satellite-Based Precipitation Datasets for Early Warning System of Extreme Storms in Hyper Arid Environment. *Climate* **2023**, *11*, 8. https://doi.org/10.3390/cli11010008.
38. Steiner, A.; Tawfik, A.; Shalaby, A.; Zakey, A.; Abdel-Wahab, M.; Salah, Z.; Solmon, F.; Sillman, S.; Zaveri, R. Climatological simulations of ozone and atmospheric aerosols in the Greater Cairo region. *Clim. Res.* **2014**, *59*, 207–228. https://doi.org/10.3354/cr01211.
39. Anwar, S.A. Constraining the Potential Evapotranspiration of Egypt Using the Regional Climate Model (RegCM4) and Climate Research Unit Dataset (CRU). *J. Biomed. Res. Environ. Sci.* **2023**, *4*, 942–952. https://doi.org/10.37871/jbres1755.
40. Anwar, S.A.; Diallo, I. On the role of a coupled vegetation-runoff system in simulating the tropical African climate: A regional climate model sensitivity study. *Theor. Appl. Clim.* **2021**, *145*, 313–325. https://doi.org/10.1007/s00704-021-03627-8.